Molecular Biology of the Cell
Vol. 16, 3411–3424, July 2005

Lamin A/C–dependent Localization of Nesprin-2, a Giant Scaffolder at the Nuclear Envelope

Thorsten Libotte,* Hafida Zaim,* Sabu Abraham,*† V. C. Padmakumar,*† Maria Schneider,* Wenshu Lu,* Martina Munck,* Christopher Hutchison,‡ Manfred Wehnert,§ Birthe Fahrenkrog,‖ Ursula Sauder,‖ Ueli Aebi,‖ Angelika A. Noegel,*† and Iakowos Karakesisoglou*

Centers for *Biochemistry and †Molecular Medicine Cologne, Medical Faculty, University of Cologne, 50931 Cologne, Germany; §Institute of Human Genetics, Ernst-Moritz-Arndt-University, 17487 Greifswald, Germany; ‡School of Biological and Biomedical Sciences, University of Durham, Durham, DH1 3LE United Kingdom; and ‖M. E. Mueller Institute, Biozentrum, University of Basel, CH-4056 Basel, Switzerland

Submitted November 17, 2004; Revised April 1, 2005; Accepted April 12, 2005
Monitoring Editor: Orna Cohen-Fix

The vertebrate proteins Nesprin-1 and Nesprin-2 (also referred to as Enaptin and NUANCE) together with ANC-1 of *Caenorhabditis elegans* and MSP-300 of *Drosophila melanogaster* belong to a novel family of α-actinin type actin-binding proteins residing at the nuclear membrane. Using biochemical techniques, we demonstrate that Nesprin-2 binds directly to emerin and the C-terminal common region of lamin A/C. Selective disruption of the lamin A/C network in COS7 cells, using a dominant negative lamin B mutant, resulted in the redistribution of Nesprin-2. Furthermore, using lamin A/C knockout fibroblasts we show that lamin A/C is necessary for the nuclear envelope localization of Nesprin-2. In normal skin where lamin A/C is differentially expressed, strong Nesprin-2 expression was found in all epidermal layers, including the basal layer where only lamin C is present. This indicates that lamin C is sufficient for proper Nesprin-2 localization at the nuclear envelope. Expression of dominant negative Nesprin-2 constructs and knockdown studies in COS7 cells revealed that the presence of Nesprin-2 at the nuclear envelope is necessary for the proper localization of emerin. Our data imply a scaffolding function of Nesprin-2 at the nuclear membrane and suggest a potential involvement of this multi-isomeric protein in human disease.

INTRODUCTION

The eukaryotic nucleus is a dynamic, highly organized organelle where several vital biological functions take place. Although its essence is undisputed, very little is known about its structural composition and architecture. The recent involvement of the nuclear envelope proteins lamin A/C and lamin-associated proteins in human diseases, however, in conjunction with the discovery of novel nuclear structural proteins has placed the nuclear architecture and its structural framework in the scientific spotlight (Burke and Stewart, 2002; Worman and Courvalin, 2002).

Until recently only microtubules and associated proteins were implicated in nuclear migratory events (Morris, 2003). Genetic evidence, however, from *Caenorhabditis elegans* suggests that nuclear migration and nuclear anchorage also involves the actin cytoskeleton because mutations in *ANC-1* affect the positioning of nuclei and mitochondria in *C. elegans* (Starr and Han, 2002). ANC-1 is a giant actin-binding dystrophin-like protein localizing to the nuclear envelope in an UNC-84 and lamin-dependent manner (Malone *et al.,* 1999; Lee *et al.,* 2002). Together with the recently discovered mammalian proteins Nesprin-1/Enaptin and Nesprin-2/NUANCE, ANC-1 of *C. elegans*, MSP-300 of *Drosophila melanogaster,* and interaptin from *Dictyostelium discoideum* are indeed the first examples of actin-binding proteins that reside at the nuclear membrane (Rivero *et al.,* 1998; Zhang *et al.,* 2001, 2002; Mislow *et al.,* 2002a; Starr and Han, 2002; Zhen *et al.,* 2002; Padmakumar *et al.,* 2004). The hallmark of the family is a single C-terminal transmembrane domain, which is separated from the N-terminal α-actinin–type actin-binding domain (ABD) by a large central coiled coil. Their C-terminus is highly conserved in evolution and responsible for nuclear envelope targeting (Zhang *et al.,* 2001; Zhen *et al.,* 2002).

Nesprin-1 and -2 are the vertebrate orthologues of ANC-1 and are encoded by two separate genes. Both genes are complex and code for several splice variants that differ in length, domain composition, and their expression pattern (Zhang *et al.,* 2001, 2002; Padmakumar *et al.,* 2004). This diversity in architecture and function is illustrated in the names that were used to describe the various products of those two genes. The small C-terminal variants of Nesprin-1 are also known as syne-1 and myne-1 (Apel *et al.,* 2000; Zhang *et al.,* 2001; Mislow *et al.,* 2002a), the ones of Nesprin-2 as syne-2 (Zhang *et al.,* 2002). The giant ABD-containing

This article was published online ahead of print in *MBC in Press* (http://www.molbiolcell.org/cgi/doi/10.1091/mbc.E04–11–1009) on April 20, 2005.

Address correspondence to: Angelika A. Noegel (noegel@uni-koeln.de).

Abbreviations used: aa, amino acids; ABD, actin-binding domain; Co-IP, coimmunoprecipitation; DAPI, 4,6-diamidino-2-phenylindole; GFP, green fluorescent protein; GST, glutathione *S*-transferase; NUANCE, *nu*cleus and *acti**n*** *c*onnecting *e*lement; Nesprins, *n*uclear *e*nvelope *sp*ectrin *r*epeat prote*ins*; siRNA, small interference RNA; X-EDMD, X-linked Emery-Dreifuss muscular dystrophy.

isoforms of the Nesprin-1 and -2 gene loci have been termed as Enaptin and NUANCE, respectively (Zhen *et al.*, 2002; Padmakumar *et al.*, 2004). For nesprin-1α, a direct binding to emerin and lamin A in vitro had been reported previously (Mislow *et al.*, 2002a, 2002b).

Because Nesprin-2 is highly homologous to Nesprin-1, we investigated whether it also associates with inner nuclear envelope components. In this report we provide evidence that Nesprin-2 binds both in vitro and in vivo to lamin A/C and emerin. We also provide data demonstrating that the localization and function of Nesprin proteins at the nuclear envelope depends on the lamin A/C network, suggesting that lamin mutations may affect the function of Nesprin-1 and -2 at the nuclear membrane. In addition, we provide evidence that Nesprin-2 localizes to both sites of the NE and is crucial for the nuclear envelope localization of emerin, thus implicating—either directly or indirectly—the Nesprin genes in human disorders.

MATERIALS AND METHODS

Construction of Plasmids

GST-K1 was made by cloning a *Bam*HI/*Sal*I PCR human Nesprin-2/NUANCE fragment (AAL33548; aa 6546–6796) into the pGEX-4T-1 vector (Amersham, Piscataway, NJ). Nesprin-2SR (AAL33548; aa 6146–6799) was generated by PCR, using the 5′-CGCTTGAGGACTGGCTCAAGTC-3′ and 5′-CTTGAGAGGAAGGAGCGCT-3′ primers, and subcloned into the ZERO blunt TOPO cloning vector (Invitrogen, Carlsbad, CA). Sequencing revealed that we accidentally introduced a stop codon at position 20,611 resulting in a protein coding for aa 6146–6799 of Nesprin-2/NUANCE. The Nesprin-2 fragment was ligated into the *Eco*RI sites of pGADT7/pGBKT7 (BD Biosciences Clontech, Palo Alto, CA), pGEX-4T-1 and pEGFP-C2 (BD Biosciences, San Diego, CA). The plasmid dnNesprin-2 is equivalent to GFP-Cterm1 (aa 6570–6883), which was published recently (Zhen *et al.*, 2002). TmNesprin-2 was amplified by PCR using the 5′-GGAATTCGGCAGCCCTACCCCTGC-3′ and 5′-CGGGATCCCTATGTGGGGGGTGGCC-3′ primers, and the amplified fragment was cloned into *Eco*RI/*Bam*HI-digested pEGFP-C1. The GFP fusion protein corresponds to aa 6833–6883 of the human Nesprin-2/NUANCE protein (AAL33548). For generating dnEnaptin we cloned an *Eco*RI/*Sal*I PCR fragment into the pEGFP-C2 plasmid, which was amplified by primers 5′-GTGAATTCCAGTTTAATTCTGACCTCAAC-3′ and 5′-GTGTCGACTTCA-GAGTGGAGGAGGACCG-3′ (corresponding to aa 8392–8749 of human Enaptin), using the mouse EST BC041779 (IMAGE) clone as a template. Yeast two-hybrid plasmids pGBT9/pGAD24-lamin A were provided by Dr. Worman (Ye and Worman, 1995). GST-Lamin A was obtained by inserting an *Eco*RI-*Sal*I-digested fragment of pGBT9 into the *Eco*RI-*Sal*I site of pGEX-4T-1. GST-N-term lamin was generated by inserting an *Eco*RI/*Sal*I-digested PCR product amplified with 5′-GAATTCATGGAGACCCCGTCCCAGCGGC-3′ and 5′-GTCGACCAGGTCACCCTCCTTCTTGGTATTG-3′, into the *Eco*RI/*Sal*I site of pGEX-4T-1. The human lamin C GST fusion proteins coil1B-delta, coil2, tail, and delta-lamin C were a generous gift of Dr. Ernoult-Lange (Dreuillet *et al.*, 2002). The human emerin recombinant protein (residues 1–222) was a generous gift of Dr. Kathy Wilson (Lee *et al.*, 2001). GFP-laminB1D2+ is described in Vaughan *et al.* (2001).

Yeast Two-hybrid Assay

The methods for performing the yeast two-hybrid assay have been described in detail elsewhere (MATCHMAKER Two-Hybrid System 2 Catalogue no. K1604–1; Clontech).

Purification of GST Fusion Proteins and In Vitro Binding Assays

The purification of GST fusion proteins and GST pulldown experiments were performed as described (Dreuillet *et al.*, 2002). For the pulldown assay using COS7 cells, lysis was performed using 50 mM Tris/HCl, pH 7.5, 150 mM NaCl, 1% Triton X-100, and protease inhibitors (Roche, Mannheim, Germany). The 100,000 × *g* supernatant of the lysate was incubated with equal amounts of GST-K1 and GST-SR fusion proteins. The solutions were incubated at 4°C overnight with GST-Sepharose beads on a roller. Samples were centrifuged and the pellets (washed three times with phosphate-buffered saline [PBS]) were analyzed by SDS-PAGE and Western blot analysis.

Blot-overlay Assay

Purified GST and *Escherichia coli* cell lysates expressing GST-lamin A were analyzed by SDS-PAGE and transferred to a membrane. After 1 h of blocking (5% milk powder in NCP buffer: 10 mM Tris/HCl, pH 8.0, 150 mM NaCl, 0.05% Tween20) the blot was incubated overnight at 4°C with the purified GST-SR recombinant fusion protein. After an extensive washing step with NCP buffer, the blot was incubated with the Nesprin-2–specific monoclonal antibody (mAb) K49–260 (described in this work) for 1 h at room temperature. The blot was washed with NCP buffer and incubated with anti-mouse IgG conjugated to peroxidase for 1 h at room temperature. After washing three times with NCP buffer, the blot was subjected to ECL detection.

siRNA Knockdown of Lamin A/C and Nesprin-2

The lamin A/C knockdown was performed as described (Harborth *et al.*, 2001). A431 cells were grown at 37°C in DMEM supplemented with 10% fetal calf serum (FCS), penicillin, and streptomycin. One day before transfection, cells were trypsinized and transferred into six-well plates. The next day the cells were washed with Opti-MEM (Life Technologies, Karlsruhe, Germany), cultured for 30 min in Opti-MEM, and transiently transfected using oligofectamine (Invitrogen) and 12 μl of a 20 μM solution of siRNA duplexes for lamin A/C per well. The specific RNA-Dimer (Harborth *et al.*, 2001; Dharmacon, Boulder, CO) targets the sequence of human lamin A/C from base 608–626. After 4 h of transfection Opti-MEM was removed and replaced with DMEM containing 10% FCS medium. After 3 d the cells were fixed and indirect immunofluorescence was performed or analyzed by SDS-PAGE and Western blot analysis. For the knockdown experiments of Nesprin-2, the oligonucleotides 5′-GATCCCCTTTGGACAATTATCCTGCATTCAAGAGATG-CAGGATAATTGTCCAAATTTTTGGAAA and 5′-AGCTTTTCCAAAAATTTG-GACAATTATCCTGCATCTCTTGAATGCAGGATAATTGTCCAAAGGG-3′ were annealed and phosphorylated in vitro and cloned into the *Bgl*II/*Hin*dIII site of the pSUPER plasmid (OligoEngine, Seattle, WA). The oligonucleotide-dimer targets the bases 595–613 of the Nesprin-2/NUANCE ABD (accession number AF435011) and allows the silencing in human and mouse as well as COS7 (African green monkey) cells. The plasmid was transfected into COS7 cells by standard transfection methods.

Immunoprecipitation of Nesprin-2 and Emerin

Subconfluent HaCaT cells were harvested and lysed in immunoprecipitation buffer (50 mM Tris/HCl, pH 7.5, 150 mM NaCl, 1% Nonidet P-40, 0.5% sodium deoxycholate, and protease inhibitors). The cell lysates were centrifuged at 12,000 × *g* for 10 min at 4°C, and the supernatants were precleared overnight with Protein A Sepharose. Lysates were centrifuged at 12,000 × *g* for 10 min, and the supernatants were mixed with the indicated antibodies (100 μl hybridoma tissue culture medium) and incubated for 2 h at 4°C. Protein A Sepharose was added to the lysates and the samples were incubated at 4°C on a rocking platform. The immunocomplexes were washed three times and subjected to SDS-PAGE and immunoblotting with the indicated antibodies.

Antibodies and Immunofluorescence Microscopy

The GST-K1 fusion protein was used for generating a mouse mAb (mAb K49–260) and a rabbit polyclonal antibody (pAb K1; Pineda, Berlin, Germany). All polyclonal Nesprin-2 and Nesprin-1/Enaptin antibodies used were purified by affinity chromatography.

Immunofluorescence studies were performed as described (Zhen *et al.*, 2002). The following antibodies were used: mouse anti-Nesprin-2 mAb K20-478 (undiluted, Zhen *et al.*, 2002), mouse anti-Nesprin-2 mAb K49–260 (undiluted), affinity-purified rabbit anti-Nesprin-2 pAb K1 (1:50), affinity-purified rabbit anti-Nesprin-1/Enaptin (1:50), mouse anti-lamin A/C (1:50, JoL2, Chemicon, Temecula, CA), rabbit anti-lamin A (1:30, Cell Signaling Technology, Beverly, MA), mouse anti-lamin A (1:40, JoL4), mouse anti-lamin B (1:40, LN42, kind gift from Frans Ramaekers and Jos Broers), mouse anti-emerin (1:50, Novacastra Laboratories, Newcastle upon Tyne, United Kingdom), mouse anti-LAP2β (1:100, BD Biosciences), goat polyclonal anti-GST antibody (Amersham Biosciences), mouse anti-GFP antibody mAb K3-184-2 (undiluted, Noegel *et al.*, 2004) and anti-β-tubulin (1:100, WA3, gift from Dr. Euteneuer), and rat a6β4 integrin antibody (1:50, gift of Dr. Niessen). Secondary antibodies for indirect immunofluorescence analysis were conjugated with Cy3 (Sigma, St. Louis, MO), FITC (Sigma), Alexa488 (Molecular Probes, Eugene, OR) and Cy5 (Chemicon). F-actin was detected with FITC-labeled phalloidin (Sigma), and nuclear staining was visualized with the DNA-specific dye DAPI (Sigma). Specimens were analyzed by wide-field fluorescence microscopy (DMR, Leica, Heidelberg, Germany) or confocal laser scanning microscopy (TCS-SP, Leica).

Immunogold Labeling

Cells were fixed in PBS, pH 7.4, containing 3% paraformaldehyde and 0.5% glutaraldehyde for 1 h, washed twice in PBS, and postfixed in 0.5% osmium tetroxide for 30 min. Next samples were dehydrated and embedded in LR White resin following the instructions of the manufacturer (Polyscience, Warrington, PA). Thin sections (50–100 nm) were mounted on Parlodion-coated Cu-grids and incubated two times for 5 min in PBS containing 2% bovine serum albumin to block unspecific binding. Next the sections were incubated with primary anti-Nesprin-2 antibodies (pAbK1 diluted 1:100 in blocking buffer, mAb K20-478 diluted 1:50 and mAb K49–260 undiluted) for 2 h (pAbK1 and mAb K20-478) and 6 h (K49–260), respectively. After washing

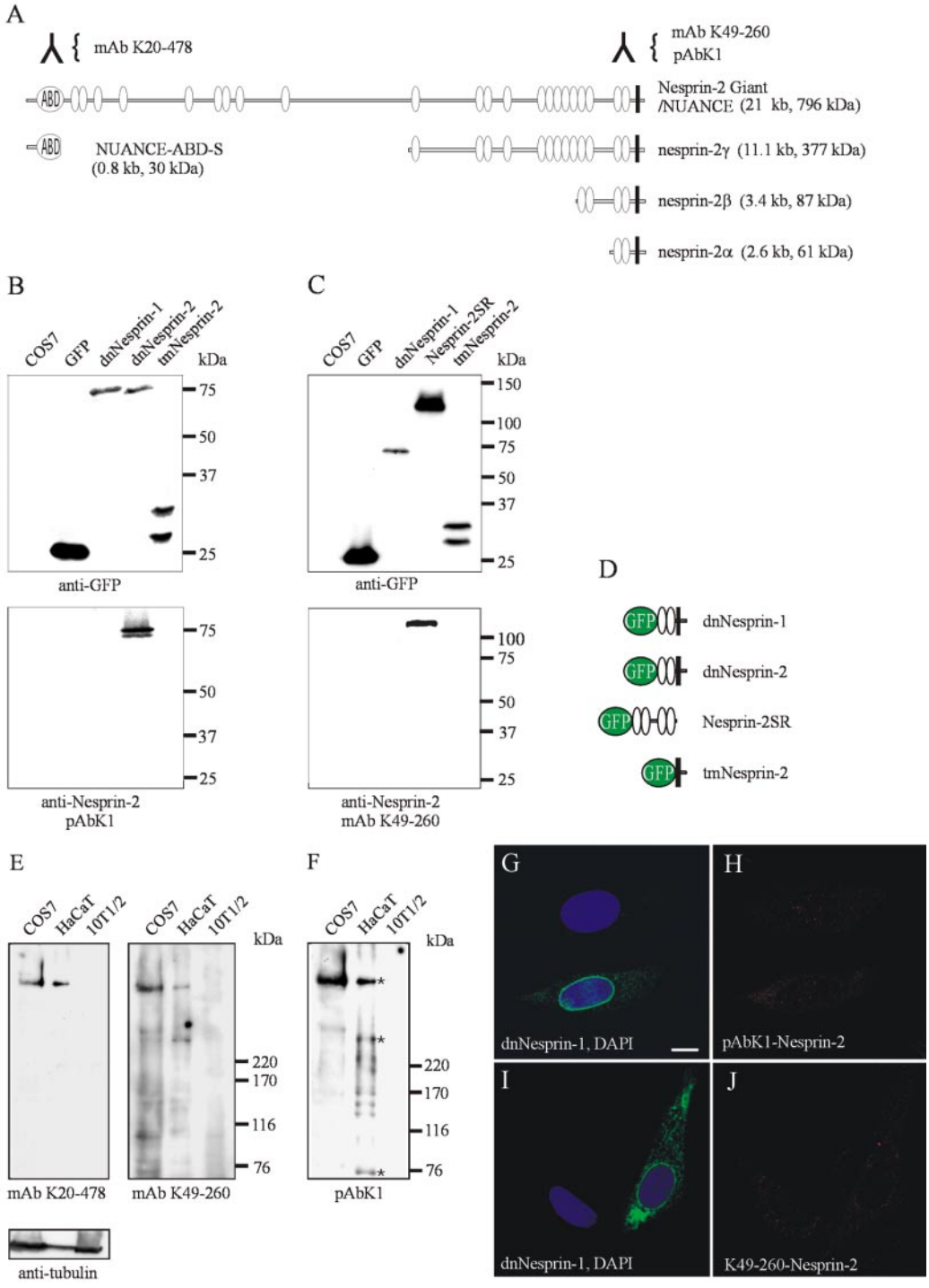

Figure 1. Splice variants of the Nesprin-2 locus and characterization of novel C-terminal Nesprin-2 antibodies. (A) Structural features of known Nesprin-2 isoforms. Nesprin-2 Giant/NUANCE consists of an N-terminal actin-binding domain (ABD), followed by several spectrin repeats (ovals) and a C-terminal transmembrane domain (black bar). Epitopes and the identity of various Nesprin-2 antibodies used in this report are indicated (inverted Y). (B and C) COS7 cells were transiently transfected with various C-terminal Nesprin GFP-fusion proteins. The COS7 cell lysates were subjected to Western blot analysis using anti-GFP–specific monoclonal antibodies to demonstrate expression of fusion proteins (top panels in B and C). Bottom panels in B and C, immunoblot analysis of the same COS7 lysates using the newly generated C-terminal polyclonal (pAb K1) and the mouse monoclonal Nesprin-2 (mAb K49-260) antibodies, verifies their specificity to the Nesprin-2 protein. (D) Schematic diagram of the GFP constructs used in this study. (E and F) COS7, HaCaT, and mouse embryonic C3H/10T1/2 cell homogenates were separated on 3–15% gradient SDS-polyacrylamide gels and blotted (Padmakumar *et al.*, 2004). Western blot analysis using the N-terminus specific Nesprin-2 antibody mAb K20-478 and the newly generated C-terminal Nesprin-2 antibodies mAb K49–260 and pAbK1, demonstrate the presence of the large 800-kDa Nesprin-2 isoform in COS7 and HaCaT cells. Nesprin-2 expression was not detected in C3H/10T1/2 fibroblast lysates. The blots shown in E originate from the same gel. The same blot was reprobed with anti-β-tubulin antibodies to illustrate equal loading. (G–J) C3H/10T1/2 fibroblasts cells transfected with the dnNesprin-1 GFP fusion protein were subjected to indirect immunofluorescence using the C-terminal Nesprin-2 antibodies pAbK1 and mAb K49–260. DAPI was used to stain nuclei. Images were taken by confocal microscopy. Bar, 10 μm.

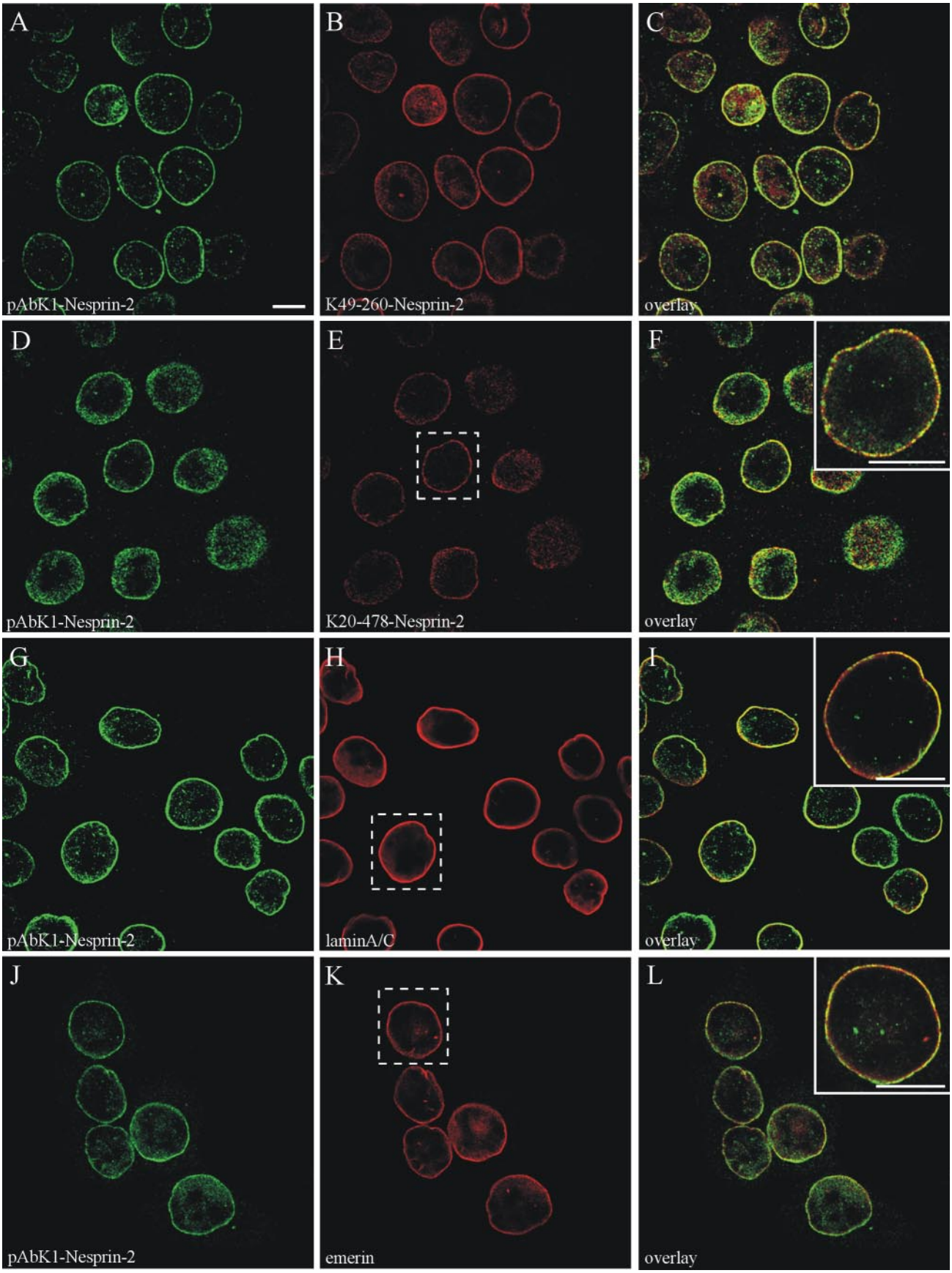
A
pAbK1-Nesprin-2
B
K49-260-Nesprin-2
C
overlay
D
pAbK1-Nesprin-2
E
K20-478-Nesprin-2
F
overlay
G
pAbK1-Nesprin-2
H
laminA/C
I
overlay
J
pAbK1-Nesprin-2
K
emerin
L
overlay

Figure 2.

with PBS, the sections were incubated with secondary goat anti-rabbit antibody conjugated to 10 nm colloidal gold (BBInternational, Cardiff, United Kingdom) and secondary goat anti-mouse antibody conjugated to 10 nm colloidal gold (BBInternational), respectively, for 1 h. After rinsing with PBS and distilled H_2O, samples were stained with 6% uranyl acetate for 1 h and lead acetate for 2 min and viewed in a LEO 910 transmission electron microscope (Zeiss, Oberkochen, Germany).

RESULTS

Generation and Characterization of C-terminal Nesprin-2 Antibodies

Nesprin-2 is encoded by a highly complex gene giving rise to several splice variants. Figure 1A provides a summary of the salient features predicted by computer analysis of all known isoforms generated by the Nesprin-2 locus. We have previously used an mAb directed against the ABD of human Nesprin-2 Giant/NUANCE isoform (mAb K20-478), which at the subcellular level stained the outer nuclear membrane (Zhen *et al.*, 2002). To allow a thorough examination and distinction of the various Nesprin-2 isoforms, we raised polyclonal and monoclonal antibodies against the last two C-terminal spectrin repeats of human Nesprin-2 (GST-K1, see Figure 3B). For a careful characterization of the antibodies we transiently transfected COS7 cells with various GFP fusion constructs harboring the C-terminal segments of Nesprin-1 and -2 (Figure 1D). Immunoblot analysis of the various COS7 cell lysates using anti-GFP antibody revealed for the GFP fusions the expected molecular masses (top panel of Figure 1, B and C). Concomitant Western blot analysis of the COS7 cell lysates demonstrated that both the polyclonal (pAbK1; bottom panel of Figure 1B) as well as the monoclonal Nesprin-2 antibodies (mAb K49–260; bottom panel of Figure 1C) reacted specifically with the Nesprin-2 GFP fusions and did not cross-react with the highly homologous Nesprin-1 protein. In addition, none of the C-terminal–directed Nesprin-2 antibodies recognized the dnNesprin-1 fusion in transiently transfected mouse embryonic C3H/10T1/2 cells (Figure 1, G–J). As shown in Figure 1, E and F, C3H/10T1/2 cells do not express Nesprin-2. Similar to mAb K20-478, both mAb K49–260 and the affinity-purified pAbK1 antibody recognized a major band of enormous size, ~800 kDa (Nesprin-2 Giant), in COS7 and HaCaT cell lysates (Figure 1, E and F). The C-terminal–specific antibodies detected consistently additional bands migrating at ~400 and 76 kDa in HaCaT lysates (Figure 1F, asterisks). The presence of the smaller N-terminally truncated Nesprin-2 isoforms in HaCaT cells was further strengthened by performing immunoprecipitation studies (see Figure 8D). The additional bands (>400 kDa) observed in COS7 cells were not always detectable; therefore, they may represent degradation products of NUANCE or cross-reactive proteins.

To evaluate the specificity of the Nesprin-2 antibodies further, we examined HaCaT cells by immunofluorescence microscopy (Figure 2, A–L). All three Nesprin-2 antibodies displayed a similar pattern and stained specifically the nuclear envelope (Figure 2, A–F). Interestingly, even the staining patterns of the pAbK1 and K20-478 antibodies were identical (see inset in Figure 2F), which is surprising considering that more than 6000 aa separate the two epitopes. Furthermore, coimmunolocalization studies using lamin A/C and emerin antibodies demonstrated a consistent overlap of these nuclear envelope proteins with Nesprin-2 (Figures 2, G–L).

Figure 2 (facing page). Nesprin-2 colocalizes with lamin A/C and emerin at the nuclear envelope of HaCaT cells. Immunolocalization studies of HaCaT cells by using anti-Nesprin-2, antilamin A/C, and anti-emerin antibodies. (A–F) HaCaT cells subjected to immunofluorescence using three different Nesprin-2 antibodies (indicated in the bottom left of each frame) demonstrate a similar nuclear localization pattern. Nesprin-2 colocalizes with lamin A/C (G–I) and emerin (J–L) at the nuclear envelope. Note the appearance of yellow in the overlay panels. Insets are higher magnifications of areas in dotted white boxes. DAPI was used to stain nuclei. Images were taken by confocal microscopy. All scale bars, 10 μm.

The C-terminus of Nesprin-2 Interacts In Vivo and in GST Pulldown Experiments with Lamin A/C

A previous study by Mislow *et al.* (2002b) reported that the last three C-terminal spectrin repeats of nesprin-1α bind directly to lamin A in vitro. Because this domain shares 46% sequence identity and 59% homology with the C-terminus of Nesprin-2 Giant/NUANCE, we examined whether Nesprin-2 also binds to lamins, using the yeast two-hybrid system. Yeast cells which were cotransformed with plasmids expressing the GAL4 DNA-binding domain fused to a C-terminal fragment of Nesprin-2 composed of the last four spectrin repeats (aa 6146–6799), and the GAL4 activation domain fused to lamin A grew on selection media and induced the β-galactosidase (Figure 3A). The yeast two-hybrid plasmids did not autoactivate the *LacZ* reporter genes themselves upon transformation into the Y190 yeast strain, demonstrating that Nesprin-2's C-terminus interacts in vivo specifically with lamin A. To verify the observations made in yeast, GST pulldown experiments were conducted using two GST-Nesprin-2 fusion proteins: GST-K1 (spectrin repeats 21 and 22) and GST-SR (spectrin repeats 19–22; Figure 3B). Equal amounts of recombinant proteins were immobilized on glutathione-agarose beads (Figure 3C, top panel) and incubated with COS7 total cell lysates. Using immunoblot analysis, lamin A/C was found to interact specifically with GST-SR but not with GST-K1 alone (Figure 3C, bottom panel).

Nesprin-2 Interacts Directly with the Common C-terminal Region of lamins A and C In Vitro

To investigate the Nesprin-2-lamin A/C-interaction in more detail we performed additional in vitro studies. Direct binding of Nesprin-2 to lamin A/C was analyzed in a blot overlay assay. Lamin A was fused to GST and its expression in *E. coli* was verified by Western blot analysis using the anti-lamin A/C antibody JoL2 (Figure 4A, right panel). Because most of the lamin A fusion protein was insoluble, we performed our experiments using the crude bacterial lysates. GST, uninduced *E. coli* cell lysate, and bacterial lysate containing GST-lamin A (Figure 4A, left panel) were blotted onto a nitrocellulose membrane and incubated with recombinant GST-SR protein. Immunodetection with mAb K49–260 gave a signal corresponding to the size of the GST-lamin fusion protein, suggesting that the C-terminal region of Nesprin-2 binds directly to lamin A (Figure 4B).

The LMNA locus codes for four proteins: lamin A, lamin C, lamin AΔ10, and the testis-specific lamin C2, which are generated through alternative splicing. Lamins A and C differ in that lamin A possesses an additional 90 aa at its C-terminus (Figure 4C; Hutchison, 2002). To map the respective lamin A/C interacting domains, we next tested specific fragments of lamin C (Figure 4, C and D) for interaction with Nesprin-2's spectrin repeats 19–22 (SR; Nesprin-2 portion of the GST-SR fusion protein after thrombin cleavage) by GST pulldown assays. We found that lamin C coil2 (aa 243–387) and lamin C tail (aa 384–566), which are contained within delta-lamin C (aa 128–572) were able to coprecipitate Ne-

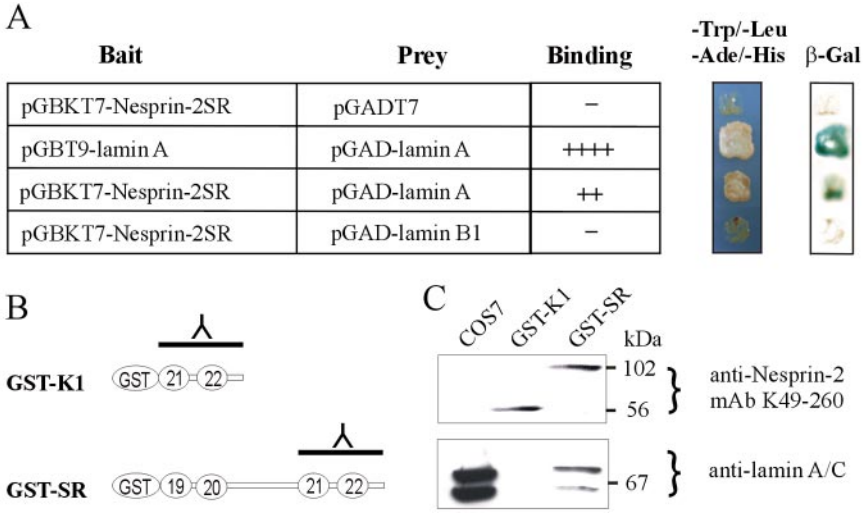

Figure 3. (A) The Nesprin-2SR fragment (aa 6146–6799) was fused to the Gal4 DNA-binding domain, whereas lamin A and B1 sequences were linked to the Gal4-activating domain. The corresponding plasmids were cotransformed into yeast cells and the interactions were assessed by the filter lift β-galactosidase assay. ++++, high blue color development; ++, weak blue color development; −, no blue color development. The growth of the yeast cells on selection media is indicated as well as β-galactosidase stainings of the colony filter lifts. GST pulldown of lamin A/C and emerin by a C-terminal Nesprin-2 fragment. (B) Schematic overview of the fusion proteins used for the GST pulldown assay of COS7 homogenates. GST-K1 consists of the last two spectrin repeats, whereas GST-SR consists of the last four spectrin repeats of Nesprin-2 Giant. The position of the epitope of the C-terminal Nesprin-2 antibody is indicated (inverted Y). (C) Immunoblotting using the C-terminus–specific Nesprin-2 mAb K49-260 demonstrates that equal amounts of the GST fusion proteins were used (top panel). COS7 cell lysates were incubated with the immobilized GST-fusion proteins. The bound proteins were subjected to SDS-PAGE followed by Western blot analysis using lamin A/C–specific antibodies (bottom panel). As a control we used a COS7 total cell lysate.

sprin-2SR, whereas with GST alone, GST-N-term (aa 1–127) and GST-coil1B-delta (aa 128–218), the SR domain stayed in the supernatant (Figure 4D, bottom panel). This finding is compatible with two independent Nesprin-2–binding domains within lamin A/C. The different binding affinities observed for lamin C coil2 and lamin C tail compared with delta-lamin C may be due to differences in folding.

The Localization of Nesprin-2 at the Nuclear Envelope Depends on the Lamin A/C Network

To pursue the interaction of Nesprin-2 and lamin A/C in vivo, we transiently expressed the mutant *Xenopus* lamin B1Δ2 in COS7 cells. This mutant protein has been previously shown to redistribute specifically A-type lamins from the lamina to nucleoplasmic granules in mammalian cells (Ellis *et al.*, 1997; Vaughan *et al.*, 2001; Figure 5, A–D). In transfected cells Nesprin-2 was located primarily in the lamin A–positive nucleoplasmic aggregates rather than at the nuclear envelope (Figure 5, E–H). A similar pattern was also evident for Nesprin-1, which no longer localized at the nuclear membrane in transfected cells (Figure 5, I–L). In agreement with what has been reported earlier (Vaughan *et al.*, 2001), the distribution of other nuclear envelope components such as lamin B and LAP2β remained unaffected and were retained exclusively at the nuclear envelope (Figure 5, M–P and Q–T, respectively). The mechanism, however, by which membrane-anchored proteins such as Nesprin-1/Nesprin-2 are being translocated to those intranuclear aggregates is unclear. To further investigate the relationship between Nesprins and lamin A/C, we investigated the localization of the Nesprin proteins in lamin A/C knockout fibroblasts (Figure 6; Sullivan *et al.*, 1999). Lamin A/C knockout fibroblasts harbor dramatic nuclear morphology changes and defects in nuclear structure (Sullivan *et al.*, 1999; Nikolova *et al.*, 2004) as well as mislocalization of various components of the nuclear envelope such as emerin. In wild-type fibroblasts the Nesprin-2 staining was confined to the nuclear envelope (Figure 6A), knockout cells, however, showed an aberrant cytoplasmic localization (Figure 6C). Similar data were obtained also for Nesprin-1, which no longer localized to the nuclear envelope in the lamin A/C knockout cells (Figure 6G). Emerin was used in our studies as a control, because its localization is known to be altered in lamin A/C–deficient fibroblasts (Sullivan *et al.*, 1999; Figure 6, F and H). Furthermore, the knockdown of lamin A/C using RNAi primers in A431 keratinocytes resulted in the mislocalization of the endogenous emerin and Nesprin-2 proteins to the cytoplasm (unpublished data). In summary, our findings demonstrate that both Nesprin-2 as well as Nesprin-1 depend on the lamin A/C network for proper nuclear envelope localization.

In Skin, Lamin C Is Sufficient for the Proper Nuclear Envelope Localization of Nesprin-2

To learn more about the lamin A/C–dependent localization of Nesprin-2, we continued our studies in skin. Skin is a stratified epithelium, where the lamin A and lamin C isoforms are differentially expressed (Venables *et al.*, 2001). Using three different Nesprin-2 antibodies, we demonstrate that Nesprin-2 is present in all living layers of the epidermis, localizing to the nuclei of the epithelial cells including the basal layer (Figure 7, A–C). Staining was strongest in epidermal keratinocytes, although weak nuclear staining was also observed for dermal fibroblasts (Figure 7, D and G, arrowheads). In contrast to lamin C,

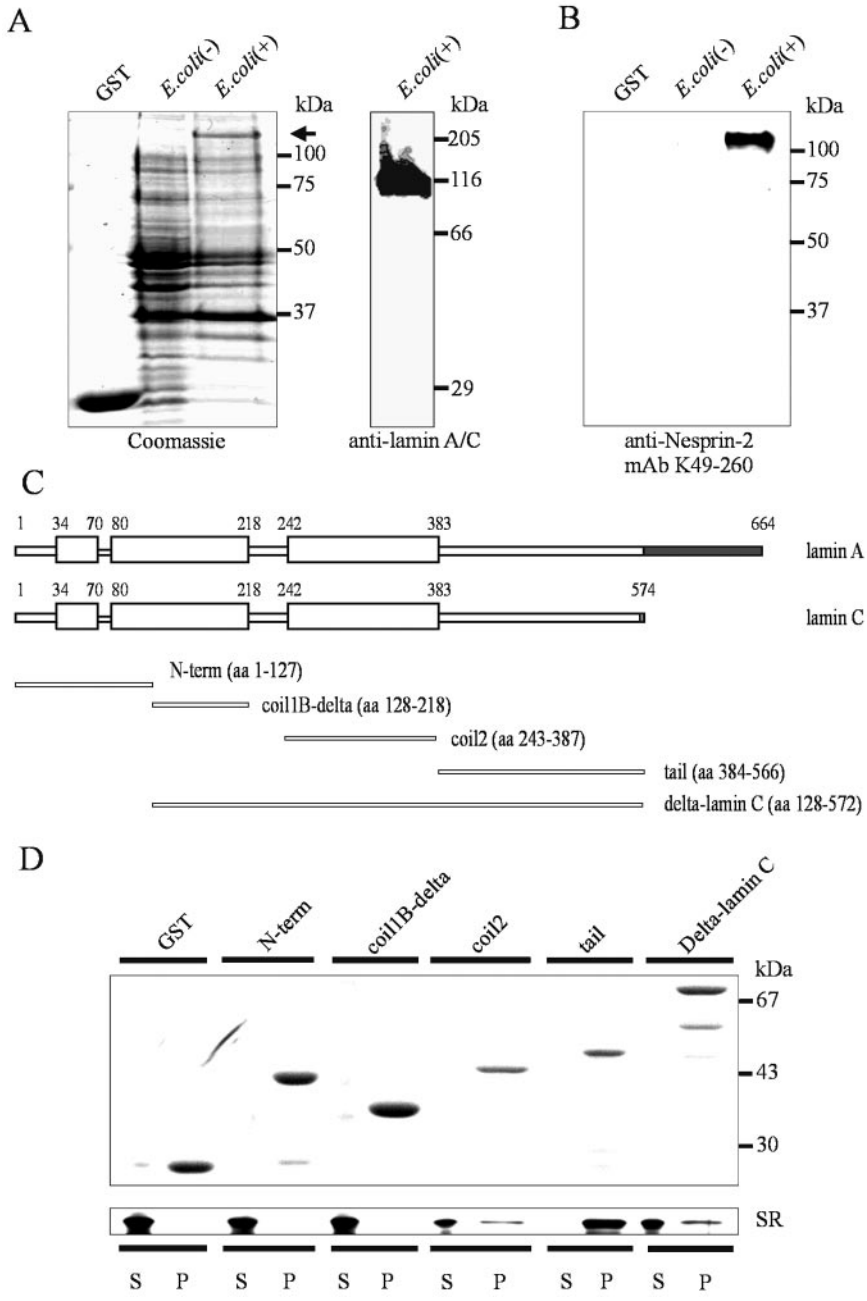

Figure 4. Nesprin-2 interacts with lamin A/C in vitro. (A) Coomassie blue–stained gel containing GST and equal amounts of uninduced (−) and induced (+) *E. coli* cell lysates expressing GST-lamin A (full-length, arrow). The expression of GST-lamin A was verified by Western blot analysis using lamin A/C (JoL2) antibodies (left panel). The proteins were blotted onto a membrane and subsequently used for blot overlay assays. (B) Blot overlay assay using the GST-SR fusion protein as a probe, followed by immunodetection with mAb K49–260 Nesprin-2 antibody. (C) Schematic overview of the domain architecture of lamin A/C and the GST-lamin C fusion proteins used for the in vitro GST pulldown assays. The unique C-terminal sequences in the lamin A and lamin C isoforms are shaded. (D) Approximately equal amounts of GST and GST lamin C fusion proteins were immobilized on agarose beads and incubated with the Nesprin-2SR recombinant protein. Samples were centrifuged and supernatant (S), pellet (P) fractions were subjected to SDS-PAGE, followed by Coomassie blue staining (top panel) to detect the GST fusion proteins and by silver staining to detect the Nesprin-2SR recombinant protein (bottom panel).

which is present in all layers of the epidermis including the basal layer (Figure 7E), lamin A is found only in few suprabasal epithelial cells (Figure 7H, arrows) and dermal fibroblasts (Figure 7H, arrowheads). Note that keratinocytes that lack lamin A staining (insets of Figure 7, H and I, asterisks) still display Nesprin-2 staining at the nuclear envelope (Figure 7I, inset). Similar data were obtained in A431 keratinocytes. Even though lamin A is not detectable in this cell line using lamin A–specific antibodies (JoL4) in immunofluorescence as well as immunoblotting, Nesprin-2 is still localizing properly to the nuclear envelope (unpublished data). Thus, our cell biological studies suggest that lamin C is sufficient for proper Nesprin-2 localization at the nuclear envelope.

Expression of a C-terminal Nesprin-2 Segment Composed of the Transmembrane Domain and the Highly Conserved Perinuclear Region Displaces Emerin from the Nuclear Envelope of COS7 Cells

In a previous study we have shown that the C-terminus of Nesprin-2 Giant/NUANCE (dnNesprin-2) is sufficient for nuclear envelope localization (Zhen *et al.*, 2002). This construct possesses spectrin repeats 21 and 22, the transmembrane domain and the highly conserved perinuclear segment of Nesprin-2 Giant. To test the significance of the two spectrin repeats in nuclear targeting, we made a shorter GFP-fusion protein, tmNesprin-2, that lacks the two spectrin repeats and harbors only the transmembrane domain and the C-terminal tail. Both fusion proteins (dnNesprin-2, tm-

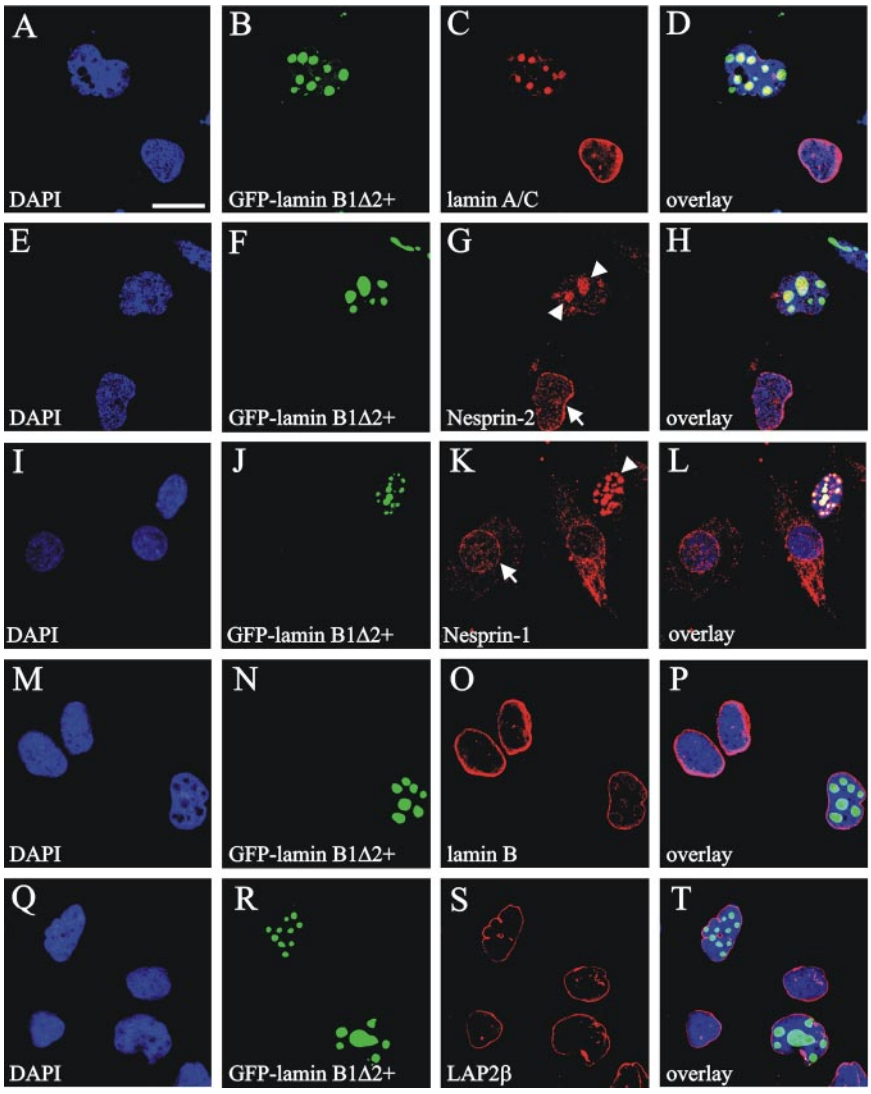

Figure 5. Nesprin-2 distribution is lamin A/C dependent. (A–T) COS7 cells were transiently transfected with a plasmid coding for the dominant negative GFP-lamin B1Δ2+ protein and subjected to immunofluorescence. Lamin A/C is redistributed into the GFP-positive nuclear patches in transfected cells and is no longer prominent at the nuclear membrane (C). Nesprin-2 (recognized by mAb K20-478) redistributes also into these GFP positive patches (G; arrowheads), whereas the endogenous protein is localized at the nuclear membrane in nontransfected cells (G, arrow). A similar pattern is also observed for Nesprin-1 (I–L). In untransfected cells Nesprin-1 is being found at the nuclear membrane (K; arrows), whereas in transfected cells Nesprin-1 colocalizes with the intranuclear GFP-patches (K; arrowheads). Endogenous lamin B and LAP2β were found to be unaffected in transfected cells and were retained at the nuclear rim (O and S, respectively). DNA was stained with DAPI. Analysis was done by confocal microscopy. Images were merged to visualize colocalization (D, H, L, P, and T). Bar, 25 μm.

Nesprin-2; Figure 1D) localized in a similar fashion to the nuclear envelope (Figure 8A, a–d and m–p, respectively) and accumulated upon overexpression also in the ER (Figure 8A, f and j). Thus, the association with the nuclear membrane is not mediated by the spectrin repeats. Moreover, upon overexpression in COS7 cells both fusion proteins displaced the endogenous Nesprin-2 proteins from the nuclear membrane (Figure 8A, c and o).

To address whether the absence of endogenous Nesprin-2 protein from the nuclear envelope will affect other compo-

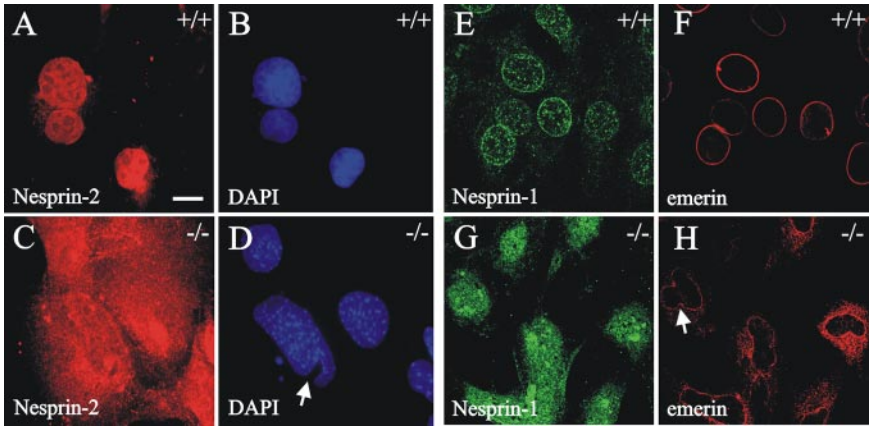

Figure 6. The distribution of Nesprins is affected in cells that do not express lamins A/C. (A–H) Wild-type and knockout lamin A/C fibroblasts were subjected to immunofluorescence using Nesprin-2 (pAbK1; A and C), Nesprin-1 (E and G, using a C-terminal Nesprin polyclonal antibody) and emerin (F and H) antibodies. Both Nesprin-2 (C) as well as Nesprin-1 (G) no longer localize at the nuclear membrane in lamin A/C knockout cells. Notice the confined nuclear envelope staining of Nesprin-2 (A) and Nesprin-1 (E) in wild-type cells. Nuclei deformations of the lamin A/C mutants are denoted by arrows. DNA was stained with DAPI. Images were taken by confocal microscopy except for A–D, which were obtained by conventional microscopy. Bar, 10 μm.

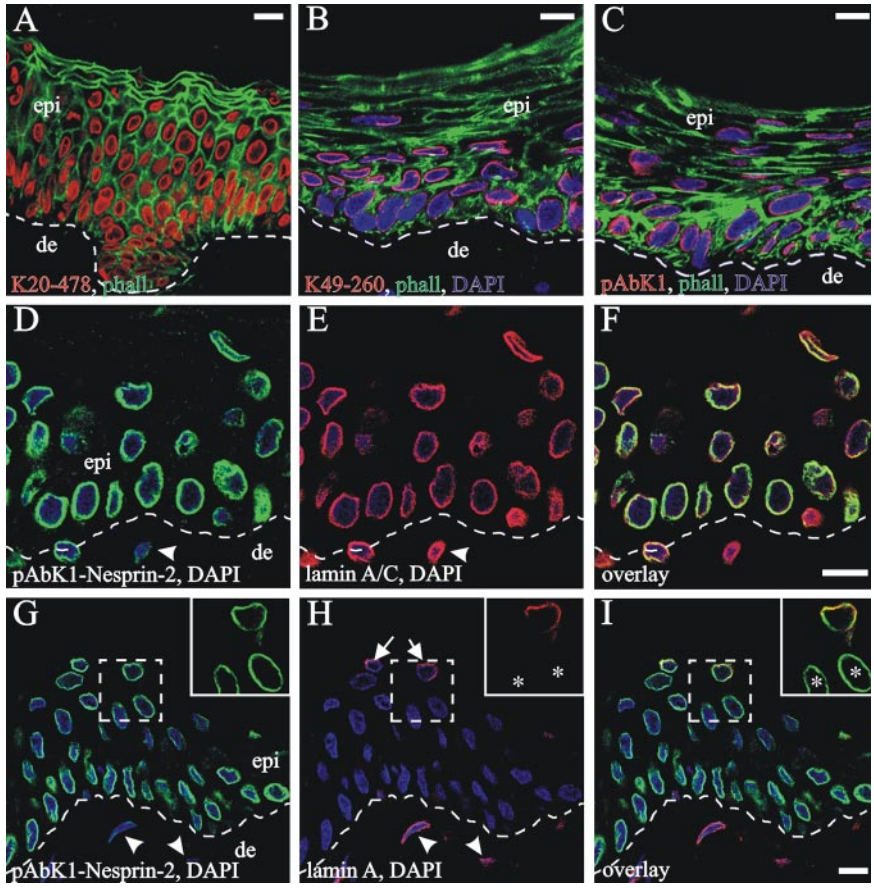

Figure 7. In human skin, lamin C is sufficient for the proper nuclear localization of Nesprin-2. (A–C) Human frozen skin sections were stained with N- and C-terminally directed Nesprin-2 antibodies as indicated in the lower left of each frame and FITC-conjugated phalloidin. Note that the antibodies share an identical nuclear staining pattern and detect Nesprin-2 throughout the living layers of the epidermis. (D–I) Human skin sections counterstained with anti-Nesprin-2- (pAbK1; D and G), JoL2- (anti-lamin A/C; E), and JoL4- (anti-lamin A; H) specific antibodies. Insets are higher magnifications of areas in dotted white boxes. Lamin A–negative keratinocytes are indicated by asterisks in the insets. Arrows indicate lamin A–positive suprabasal keratinocytes, whereas arrowheads indicate lamin A–positive dermal fibroblasts (H). Dermal fibroblasts are indicated by arrowheads; notice the reduced Nesprin-2 staining in the dermal fibroblasts (D and G; arrowheads). The dotted line denotes the basement membrane, which was visualized by counterstaining with a6β4 antibodies and a Cy5-conjugated secondary antibody. DNA was stained with DAPI Images were taken by confocal microscopy. epi, epidermis; de, dermis. All scale bars, 10 μm.

nents of the inner nuclear membrane, we performed indirect immunofluorescence stainings of transfected cells using antibodies against lamin A/C and emerin. Although the appearance and the overall pattern of lamin A/C at the nuclear membrane was not affected by the overexpression of either dnNesprin-2 (Figure 8A, e–h) or tmNesprin-2 (unpublished data) GFP fusion proteins, we found drastic changes in the emerin pattern in tmNesprin-2–transfected cells. In sharp contrast to the dnNesprin-2 protein (Figure 8A, i–l), only the tmNesprin-2 construct (Figure 8A, q–t) was able to mislocalize emerin from the nuclear membrane. Emerin displayed strong nuclear staining in untransfected COS7 cells; however, the protein no longer localized to the nuclear membrane and accumulated in cytoplasmic granules in 60% of COS7 cells that express tmNesprin-2. Around 5% of transfected cells did not display any alterations of emerin, and another 35% displayed a partial mislocalization of emerin to the cytoplasm. The numbers provided where obtained by counting 200 transiently transfected cells.

Nesprin-2 Interacts Directly with Emerin In Vitro and in HaCaT Cells

To examine whether Nesprin-2 and emerin are interacting with each other, we conducted GST pulldown experiments. Equal amounts of recombinant proteins were immobilized on glutathione-agarose beads (Figure 8B, top panel) and incubated with COS7 total cell lysates. Using immunoblot analysis, emerin was found to interact specifically with GST-K1 (Figure 8B, lower panel). To further investigate whether Nesprin-2 associates directly with emerin, we performed GST pulldown experiments using recombinant emerin protein. Our results show that in contrast to GST, GST-K1 specifically interacted with emerin (Figure 8C). Nesprin-2's interaction with emerin was further examined in vivo by immunoprecipitation using the mAb K49–260 antibody. This antibody was able to coimmunoprecipitate specifically the various Nesprin-2 isoforms and emerin from HaCaT cell lysates (Figure 8D). In addition, the immunoblot analysis using the pAbK1 Nesprin-2 antibody on the CoIP samples further underlined the specificity of the C-terminal Nesprin-2 antibodies.

Ablation of Nesprin-2 Expression in COS7 Cells Using the siRNA Technology Affects the Nuclear Envelope Localization of Emerin

Our immunofluorescence studies using dominant negative Nesprin-2 constructs revealed an unexpected relationship between Nesprin-2 and emerin. The mechanism, however, by which those dominant negative Nesprin-2 proteins act has not been studied so far in detail. In addition, the Nesprin-2 interactions in the perinuclear space have not been elucidated at the biochemical level. Therefore it cannot be excluded that the effects on emerin may have been indirect.

To unequivocally demonstrate that the emerin mislocalization was caused due to the absence of Nesprin-2, we performed siRNA Nesprin-2 knockdown experiments in COS7 cells. For this purpose, we designed RNA duplexes against the N-terminus of Nesprin-2 Giant/NUANCE (see *Materials and Methods*). We chose for our studies COS7 cells because they express only the large ABD-containing isoforms and lack the small C-terminal isoforms (see Figure 1, E and F) in order to accomplish the complete knockdown of

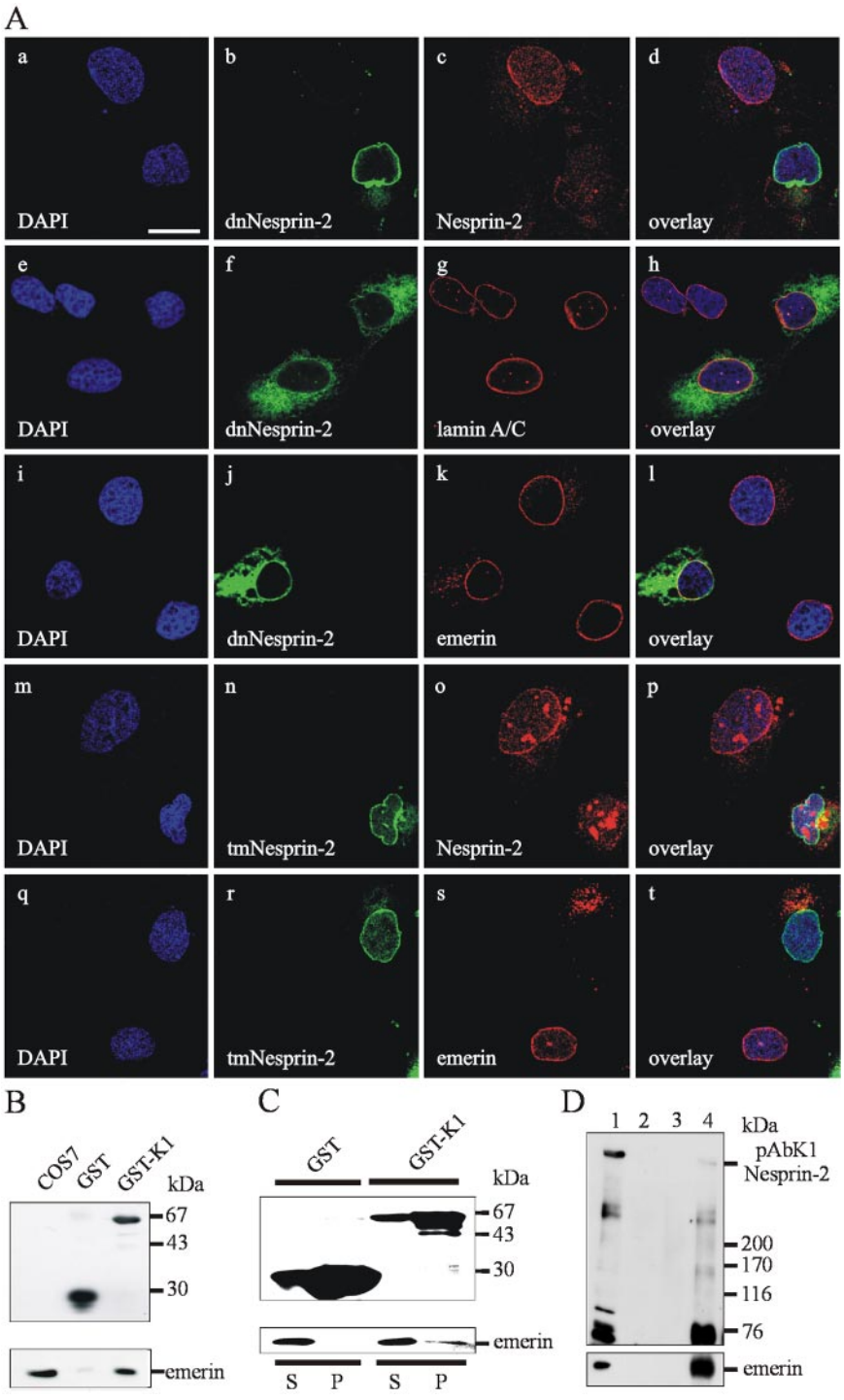

Figure 8. Dominant negative interference with the Nesprin-2 localization in COS7 cells influences the localization of emerin. (A) COS7 cells were transiently transfected with plasmids allowing expression of the GFP-tagged C-terminal Nesprin-2 dominant negative polypeptides dnNesprin-2 (a–l) and tm-Nesprin-2 (m–t). The constructs used are described in *Material and Methods* and a schematic overview of their composition is shown in Figure 1D. Immunofluorescence studies were performed using Nesprin-2 (c and o), lamin A/C (g), and emerin antibodies (k and s). Although both constructs localize to the nuclear envelope and displace the endogenous Nesprin-2 proteins (c and o), a mislocalization of emerin in the cytoplasm is observed only for the tmNesprin-2 GFP construct (s). The cells were fixed with paraformaldehyde. DNA was stained with DAPI. Analysis was done by confocal microscopy. Images were merged to visualize colocalization (d, h, l, p, and t). Bar, 25 μm. (B) Emerin associates directly with Nesprin-2 in vitro. GST and GST-K1 fusion proteins were immobilized on glutathione agarose beads and were incubated either with COS7 cell lysates (B) or with recombinant emerin protein (C). Samples were centrifuged and supernatant (S) and pellet (P) fractions were subjected to SDS-PAGE, followed by immunoblot analysis to detect the GST fusions proteins (top panels) and emerin (bottom panels). (D) CoIP of Nesprin-2 and emerin from HaCaT cell lysates. HaCaT cells were lysed, and the supernatants were incubated with anti-Nesprin-2 (mAb K49-260) antibodies. The immunocomplexes were analyzed by SDS-PAGE and subjected to immunoblotting with anti-Nesprin-2 (pAbK1) and emerin antibody. Lane 1, total cell lysate; lane 2, lysate precipitated with Protein A Sepharose beads; lane 3, lysate precipitated with anti GFP antibody on Protein A Sepharose beads; lane 4, lysate precipitated with anti-Nesprin-2 antibody on Protein A/G Sepharose beads.

Nesprin-2. COS7 cells were transiently transfected with the pSUPER plasmid and after 3 d of culturing the cells were subjected to Western blot (Figure 9A) and immunofluorescence analysis (Figure 9, B–J). Lysates of transiently transfected COS7 cells contained only minor amounts of Nesprin-2, illustrating the efficacy of Nesprin-2 silencing. In sharp contrast, however, lamin A/C, emerin and tubulin levels were comparable to wild-type (Figure 9A, lower panels). Confocal microscope analysis of the transfected COS7 cells revealed that the RNA interference of the N-terminal Nesprin-2 sequences results in the complete absence of the Nesprin-2 staining pattern with both N- as well as C-terminal directed Nesprin-2 antibodies (Figure 9, B and C, asterisks). In many transfected COS7 cells the Nesprin-2 staining was absent from the nuclear membrane and what little staining that remained was cytoplasmic (Figure 9, B, E, and H, asterisks). Cells, where Nesprin-2 was absent from the nuclear membrane no longer harbored emerin at the nuclear envelope. Emerin was found primarily in aggregates that were dispersed throughout the cytoplasm (Figure 9I, arrowheads).

To evaluate the knockdown of Nesprin-2 in COS7 cells, we performed measurements of the fluorescence intensity

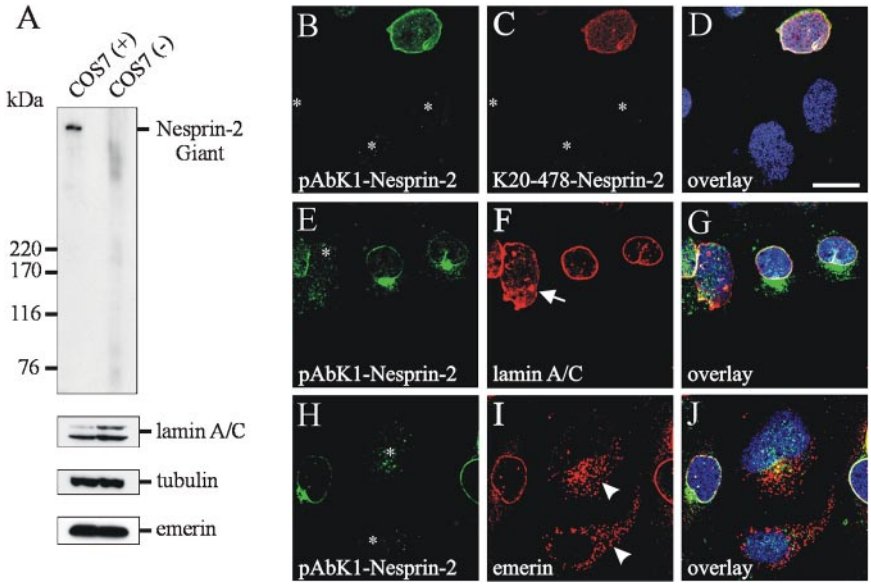

Figure 9. The emerin distribution is affected in cells where Nesprin-2 expression has been silenced by siRNA. (A) COS7 cells were transiently transfected with the pSUPER plasmid expressing RNA duplexes against the N-terminus of Nesprin-2. Cell lysates were subjected to Western blot analysis using Nesprin-2 (pAbK1), lamin A/C, emerin and tubulin antibodies, illustrating the efficiency of the Nesprin-2 knockdown. The distribution of Nesprin-2 (B, E, and H; using pAbK1 and C; using K20-478), lamin A/C (F), and emerin (I) was investigated by indirect immunofluorescence in knockdown Nesprin-2 COS7 cells (indicated by an asterisk). In knockdown Nesprin-2 cells, lamin A/C remained at the nuclear envelope (F, arrow), whereas emerin was dispersed in cytoplasmic aggregates (I; arrowheads). Cells were fixed with paraformaldehyde. DNA was stained with DAPI. Analysis was done by confocal microscopy. Images were merged to visualize colocalization (D, G, and J). Bar, 25 μm.

(Nesprin-2)/nucleus size (ImageJ, NIH Image) in cells with an abnormal emerin distribution and compare it with cells exhibiting proper emerin localization. We found that the Nesprin-2 fluorescence intensity is reduced by 40% in cells with an abnormal emerin distribution. A paired *t* test showed that the reduction of fluorescence intensity/nucleus size ($n = 30$, $p < 0001$) is significant. By contrast, lamin A/C remained in the nuclear lamina (Figure 9F, arrow).

To investigate whether Nesprin-2 distribution was dependent on emerin, immunofluorescence studies were performed on dermal fibroblasts null for emerin (Figure 10, A and E–G) from patients suffering from X-EDMD caused by the *STA* g631 del TCTAC mutation (Hoeltzenbein *et al.*, 1999). As shown in Figure 10A (top panel), Nesprin-2 is expressed in both wild-type and mutant human dermal fibroblasts and represented predominantly by its large 800-kDa isoform. Nesprin-2 displayed a strong nuclear envelope staining pattern in wild-type fibroblast cells (Figure 10D, arrowheads). Although some mutant fibroblasts did exhibit increased cytoplasmic staining for Nesprin-2, the majority of the protein remained at the nuclear envelope (Figure 10G, arrowheads). Thus, our data strongly suggest that the emerin localization to the nuclear envelope in COS7 cells depends on Nesprin-2.

Nesprin-2 Is a Component of the Outer and Inner Nuclear Membrane in HaCat Cells

The association of Nesprin-2 with inner nuclear proteins such as lamin A/C and emerin strongly suggested its presence within the nucleus. To elucidate the exact Nesprin-2 topology at the nuclear membrane we performed immunoelectron microscopy in HaCaT cells using all three Nesprin-2 antibodies. Prominent immunogold decoration of the NE was observed with all Nesprin-2 antibodies (Figure 11, A–C); however, the strongest labeling was observed with the pAbK1 polyclonal antibody. Nesprin-2 labeling appeared in clusters, which were observed on the outer (Figure 11A, black arrows) as well as the inner nuclear membrane (Figure 11A, open arrowheads). A similar staining pattern was observed with the monoclonal N- and C-terminal Nesprin-2 antibodies (Figure 11, B and C, respectively). Quantitation of the immunogold particles demonstrates that more gold particles are detected within the nucleus than on the cytoplasmic side of the NE (Figure 11D).

DISCUSSION

The data presented here demonstrate that Nesprin-2 associates directly both in vitro and in vivo with lamin A/C and

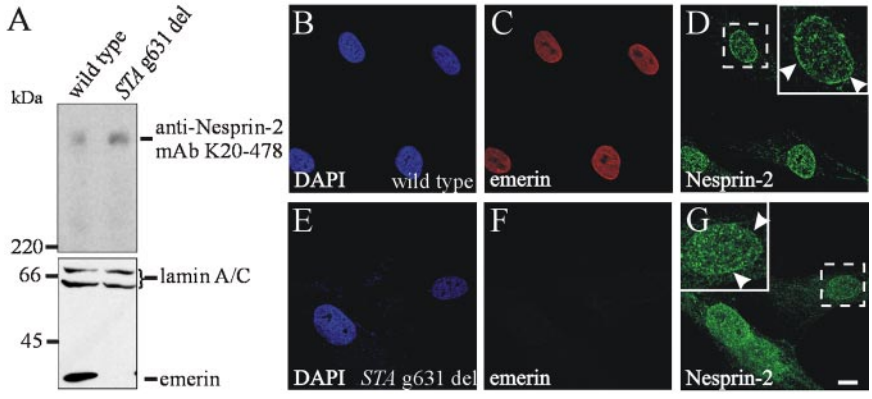

Figure 10. Emerin is not necessary for the NE localization of Nesprin-2 in dermal fibroblasts. (A) Immunoblot analysis of wild-type and emerin-deficient (*STA* g631 del) human fibroblasts lysates using anti-Nesprin-2 (mAb K20-478), lamin A/C- and emerin-specific antibodies. Wild-type (B–D) and emerin-deficient cells (E–G) were subjected to immunofluorescence using antibodies against Nesprin-2 (mAb K20-478) and emerin. Insets are higher magnifications of areas in dotted white boxes. Arrowheads denote the Nesprin-2 staining at the nuclear envelope. Note the persistence of the nuclear staining pattern of Nesprin-2 in the mutant cells (G). The images were taken by confocal microscopy. Nuclei were visualized by DAPI staining. Bar, 10 μm.

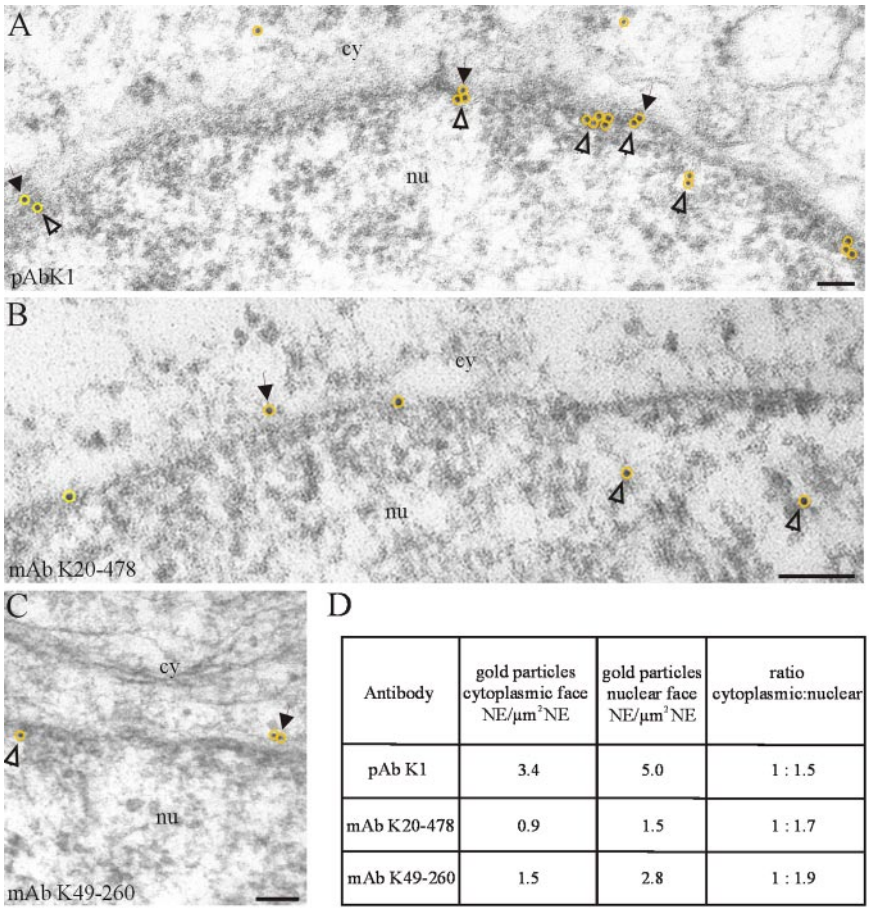

Antibody	gold particles cytoplasmic face NE/μm²NE	gold particles nuclear face NE/μm²NE	ratio cytoplasmic:nuclear
pAb K1	3.4	5.0	1 : 1.5
mAb K20-478	0.9	1.5	1 : 1.7
mAb K49-260	1.5	2.8	1 : 1.9

Figure 11. Immunogold EM examination of Nesprin-2. In HaCaT cells pAbK1 (A), mAb K20-478 N-terminal (B) and mAb K49–20 C-terminal Nesprin-2–specific antibodies (C) recognize nuclear (open arrowheads) as well as cytoplasmic (black arrows) Nesprin-2 protein at the NE. The gold particles appear often in clusters (A) and are marked with yellow circles. Quantification of Nesprin-2 antibody labeling at the nuclear envelope (D). nu, nucleus; cy, cytoplasm. All scale bars, 100 nm.

emerin. These findings are consistent with previous reports regarding Nesprin-2's homologue Nesprin-1. Mislow *et al.* (2002b) showed that nesprin-1α, a C-terminal isoform of Nesprin-1 Giant/Enaptin, interacts directly with emerin and lamin A in vitro. In sharp contrast to emerin, which is not required for the proper subcellular distribution of Nesprin-2, the selective alteration and ablation of the lamin A/C network has profound effects on the nuclear envelope localization of Nesprin-2. Our biochemical observations and immunohistochemical data on skin suggest that lamin C is sufficient for Nesprin-2 binding and its proper localization at the nuclear envelope. These data are in agreement with a recent report, in which human fibroblasts that carry the homozygous missense mutation Y259X in lamin A/C exhibit an aberrant nesprin-1α and emerin localization. Interestingly, the expression of lamin C in the mutant cells was sufficient to restore the proper anchorage of both emerin and nesprin-1α at the nuclear envelope (Muchir *et al.*, 2003).

The scaffolding aspects of lamin in relation to Nesprin-2 seem to be evolutionarily conserved and have been also reported in *C. elegans*. The localization of ANC-1 in *C. elegans* at the nuclear envelope requires lamin and also the inner nuclear membrane protein UNC-84 (Lee *et al.*, 2002; Starr and Han, 2002), suggesting a bridging model in which the outer nuclear membrane protein ANC-1 interacts through a "structural bridge" composed of UNC-84 and associated proteins with the nuclear lamina (Starr and Han, 2003). Interestingly two UNC-84 orthologues, SUN1 and SUN2, have been identified in humans (Malone *et al.*, 1999; Hodzic *et al.*, 2004). Their presence suggests that an indirect anchorage mechanism to the nuclear lamina may exist also for Nesprins localized at the outer nuclear membrane in addition to the direct interaction demonstrated here.

Although the biochemical details regarding the proteins implicated in such a model are still missing, our data propose that lamin A/C mutations may disrupt the localization and function of Nesprin-2 at the nuclear envelope. Mutations in human lamins cause a variety of disorders affecting various tissues including skeletal muscle (Burke and Stewart, 2002; Hutchison, 2002; Worman and Courvalin, 2002). Interestingly, both Nesprin-1 as well Nesprin-2 isoforms are expressed in skeletal muscle and genetic data from *D. melanogaster* indicate a requirement of the fly orthologue MSP-300 in embryonic muscle morphogenesis (Rosenberg-Hasson *et al.*, 1996). Therefore, lamin mutations may weaken or disrupt the interactions with Nesprins, resulting in loss-of-function mutants. Further data will be needed to prove an involvement of Nesprin-1 and -2 in laminopathies.

Our results suggest a novel Nesprin-2–based mechanism by which emerin is properly localized to the nuclear membrane. The observation, however, that the dominant negative tmNesprin-2 construct or the Nesprin-2 silencing mislocalizes emerin is very surprising, considering that emerin is able to bind by itself to various nuclear proteins, including lamin A/C (Bengtsson and Wilson, 2004). How does the absence of Nesprin-2 from the nuclear envelope influence emerin in cells exhibiting a normal expression and localization of lamin A/C? One possible scenario is that Nesprin-2 recruits and stabilizes emerin at the nuclear envelope through a direct interaction, a scenario, which is substantiated by our results showing a direct association of the last two C-terminal spectrin repeats of Nesprin-2 with emerin.

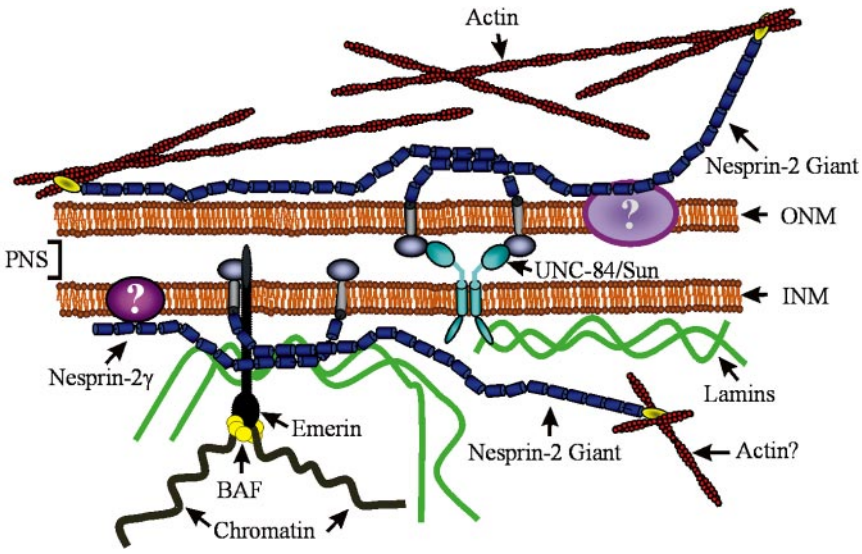

Figure 12. A model, illustrating the interactions of Nesprin-2 Giant and its isoforms (Nesprin-2γ) with various cytoplasmic and nucleoplasmic components at the nuclear membrane (see *Discussion* for details). Unknown complexes, which may include peripheral (members of the 4.1 protein family) as well as integral elements of the nuclear membrane are depicted as large ovals. ONM, outer nuclear membrane; INM, inner nuclear membrane; PNS, perinuclear space; BAF, barrier-to-autointegration factor.

Our model is further strengthened by the data we obtained from the expression of the dnNesprin-2 GFP-fusion protein in COS7 cells. In contrast to tmNesprin-2, this polypeptide contains the last two C-terminal spectrin repeats, which bind to emerin in vitro. Although both proteins can displace Nesprin-2, a profound effect on emerin is only observed with the tmNesprin-2 construct where the emerin binding site is missing. Interestingly, such an interaction has also been described for the C-terminal spectrin repeats of nesprin-1α. Although the amino-terminal half of nesprin-1α (spectrin repeats 1–5) was found to bind with high-affinity to emerin (53 nM), a week association (250 nM) to emerin was demonstrated for the last three spectrin repeats (spectrin repeats 5–7) of the nesprin-1α molecule (Mislow *et al.*, 2002b). Furthermore, our data provide a clear explanation for a previous study, which demonstrated that dominant negative mutants of lamin A/C cause emerin to accumulate in cytoplasmic granules (Vaughan *et al.*, 2001). The authors concluded that lamin A/C is essential for anchorage of emerin to the inner nuclear membrane. Our experiments showed that in addition those constructs affect also the localization of Nesprins at the nuclear envelope, suggesting that this event may lead to the accumulation of emerin in the cytoplasm. Even though much has been reported about the nuclear-membrane targeting determinants of emerin and its multiple binding partners, the exact mechanism still remains unclear (Fairley *et al.*, 1999; Östlund *et al.*, 1999; Tsuchiya *et al.*, 1999; Lee *et al.*, 2001). Interestingly, emerin was recently identified as a pointed-end actin-capping protein (Holaska *et al.*, 2004). Therefore, emerin and Nesprin complexes may be involved additionally in the assembly and the organization of nuclear actin structures.

In a recent study, Zhen *et al.* (2002) using digitonin extraction methods reported the presence of Nesprin-2 Giant/NUANCE at the outer nuclear membrane but also in the nucleus. Here, we showed that Nesprin-2 localizes also to the inner nuclear membrane. This suggests that the Nesprin-2 and the orthologous Nesprin-1 proteins function both inside and outside the nucleus, enabling them to act as molecular bridges connecting the cytoskeleton with the nuclear matrix, intranuclear actin, and spectrin-associated proteins such as members of the 4.1 protein superfamily (Figure 12). Indeed immunogold labeling analysis of nesprin-1 in myoblast cells demonstrated its presence at the nuclear envelope and also within the nucleus, where it colocalized with regions of heterochromatin (Zhang *et al.*, 2001). Current models, would favor the presence of the smaller N-terminally truncated isoforms within the inner nuclear membrane, whereas the bigger ABD-containing isoforms would preferentially be components of the outer nuclear membrane (Soullam and Worman, 1995). The presence, however, of the giant ABD-containing isoforms at the inner nuclear membrane suggests that alternative sorting mechanisms other than the known lateral diffusion through the nuclear pores must exist to establish such a localization.

In closing, our present study establishes linkages and interconnections between Nesprins, lamin A/C, and the emerin molecules (Figure 12), which have been implicated in a wide range of tissue-specific diseases. Genetic data using the embryonic stem cell technology will shed some light on the potential involvement of Nesprins in human genetic diseases and reveal whether they correspond to the "biological Atlas" of the cell holding up and keeping the nucleus (universe) in position. One aspect is, however, already apparent: eukaryotic nuclei use giant scaffolding proteins that, similar to cytoplasmic linkers, have the capacity to cross-bridge various architectural elements and structurally organize membranes. With an 800-kDa Nesprin-2, or an 1-MDa Nesprin-1 protein there is still much to learn about the putative interactions and their biology. Revealing their function remains a great challenge since they are the largest molecules of the α-actinin superfamily and of complex structural organization.

Note added in proof. While this paper was under review, Zhang *et al.* (2005) published an article demonstrating the existence of various Nesprin-2 isoforms within the nucleus, the outer nuclear membrane, and various cytoplasmic compartments. These data suggest that nesprin-2 isoforms may link various membranous compartments including the nucleus to the actin cytoskeleton. The authors showed that the smaller Nesprin-2 isoforms colocalize and bind to lamin A/C and emerin at the inner nuclear membrane and require lamin A/C for proper localization in SW-13 cells. Those associations allowed the authors to suggest that a Nesprin-based mechanism may explain how disruption/s of NE constituents leads to muscle dysfunction.

ACKNOWLEDGMENTS

We thank Drs. M. Ernoult-Lange, K. L. Wilson, F. Ramaekers, J.L.V. Broers, H. J. Worman, C. L. Stewart, B. Burke, H. Herrmann, R. Foisner, C. Niessen, and C. Mauch for providing reagents and Rolf Müller for providing the GST-K1 recombinant protein. This work was supported by a grant from the Center for Molecular Medicine Cologne, the Deutsche Forschungsgemeinschaft (SFB 589) and the Maria-Pesch-Foundation. M.W. was supported by a grant of the Bundesministerium für Bildung und Forschung 01GM0302.

REFERENCES

Apel, E. D., Lewis, R. M., Grady, R. M., and Sanes, J. R. (2000). Syne-1, a dystrophin- and Klarsicht-related protein associated with synaptic nuclei at the neuromuscular junction. J. Biol. Chem. *275*, 31986–31995.

Bengtsson, L., and Wilson, K. L. (2004). Multiple and surprising new functions for emerin, a nuclear membrane protein. Curr. Opin. Cell Biol. *16*, 1–7.

Burke, B., and Stewart, C. L. (2002). Life at the edge: the nuclear envelope and human disease. Nat. Rev. Mol. Cell. Biol. *3*, 575–585.

Dreuillet, C., Tillit, J., Kress, M., and Ernoult-Lange, M. (2002). In vivo and in vitro interaction between human transcription factor MOK2 and nuclear lamin A/C. Nucleic Acids Res. *30*, 4634–4642.

Ellis, D. J., Jenkins, H. E., Whitfield, W.G.F., and Hutchison, C. J. (1997). GST-lamin fusion proteins act as dominant negative mutants in *Xenopus* egg extract and reveal the function of the lamina in DNA replication. J. Cell Sci. *110*, 2507–2518.

Fairley, E. A., Kendrick-Jones, J., and Ellis, J. A. (1999). The Emery-Dreifuss muscular dystrophy phenotype arises from aberrant targeting and binding of emerin at the inner nuclear membrane. J. Cell Sci. *112*, 2571–2582.

Harborth, J., Elbashir, S. M., Bechert, K., Tuschl, T., and Weber, K. (2001). Identification of essential genes in cultured mammalian cells using small interfering RNAs. J. Cell Sci. *114*, 4557–4565.

Hodzic, D. M., Yeater, D. B., Bengtsson, L., Otto, H., and Stahl, P. D. (2004). Sun2 is a novel mammalian inner nuclear membrane protein. J. Biol. Chem. *279*, 25805–25812.

Hoeltzenbein, M., Karow, T., Zeller, J. A., Warzok, R., Wulff, K., Zschiesche, M., Herrmann, F. H., Grosse-Heitmeyer, W., and Wehnert, M. S. (1999). Severe clinical expression in X-linked Emery-Dreifuss muscular dystrophy. Neuromuscul. Disord. *9*, 166–170.

Holaska, J. M., Kowalski, A. K., and Wilson, K. L. (2004). Emerin caps the pointed end of actin filaments: evidence for an actin cortical network at the nuclear inner membrane. PLoS Biol. *2*, E231.

Hutchison, C. J. (2002). Lamins: building blocks or regulators of gene expression? Nat. Rev. Mol. Cell. Biol. *3*, 848–858.

Lee, K. K., Haraguchi, T., Lee, R. S., Koujin, T., Hiraoka, Y., and Wilson, K. L. (2001). Distinct functional domains in emerin bind lamin A and DNA-bridging protein BAF. J. Cell Sci. *114*, 4567–4573.

Lee, K. K., Starr, D., Cohen, M., Liu, J., Han, M., Wilson, K. L., and Gruenbaum, Y. (2002). Lamin-dependent localization of UNC-84, a protein required for nuclear migration in *Caenorhabditis elegans.* Mol. Biol. Cell *13*, 892–901.

Malone, C. J., Fixsen, W. D., Horvitz, H. R., and Han, M. (1999). UNC-84 localizes to the nuclear envelope and is required for nuclear migration and anchoring during *C. elegans* development. Development *126*, 3171–3181.

Mislow, J.M.K., Kim, M. S., Davis, D. B., and McNally, E. M. (2002a). Myne-1, a spectrin repeat transmembrane protein of the myocyte inner nuclear membrane, interacts with lamin A/C. J. Cell Sci. *115*, 61–70.

Mislow, J.M.K., Holaska, J. M., Kim, M. S., Lee, K. K., Segura-Totten, M., Wilson, K. L., and McNally, E. M. (2002b). Nesprin-1alpha self-associates and binds directly to emerin and lamin A in vitro. FEBS Lett. *525*, 135–140.

Morris, N. R. (2003). Nuclear positioning: the means is at the ends. Curr. Opin. Cell Biol. *15*, 54–59.

Muchir, A., van Engelen, B. G., Lammens, M., Mislow, J. M., McNally, E., Schwarz, K., and Bonne, G. (2003). Nuclear envelope alterations in fibroblasts from LGMD1B patients carrying nonsense Y259X heterozygous or homozygous mutation in lamin A/C gene. Exp. Cell Res. *291*, 352–362.

Nikolova, V. *et al.* (2004). Defects in nuclear structure and function promote dilated cardiomyopathy in lamin A/C-deficient mice. J. Clin. Invest. *113*, 357–369.

Noegel, A. A., Blau-Wasser, R., Sultana, H., Muller, R., Israel, L., Schleicher, M., Patel, H., and Weijer, C. J. (2004). The cyclase-associated protein CAP as regulator of cell polarity and cAMP signalling in *Dictyostelium*. Mol. Biol. Cell *15*, 934–945.

Östlund, C., Ellenberg, J., Hallberg, E., Lippincott-Schwartz, J., and Worman, H. J. (1999). Intracellular trafficking of emerin, the Emery-Dreifuss muscular dystrophy protein. J. Cell Sci. *112*, 1709–1719.

Padmakumar, V. C., Abraham, S., Braune, S., Noegel, A. A., Tunggal, B., Karakesisoglou, I., and Korenbaum, E. (2004). Enaptin, a giant actin-binding protein, is an element of the nuclear membrane and the actin cytoskeleton. Exp. Cell Res. *295*, 330–339.

Rivero, F., Kuspa, A., Brokamp, R., Matzner, M., and Noegel, A. A. (1998). Interaptin, an actin-binding protein of the alpha-actinin superfamily in *Dictyostelium discoideum*, is developmentally and cAMP-regulated and associates with intracellular membrane compartments. J. Cell Biol. *142*, 735–750.

Rosenberg-Hasson, Y., Renert-Pasca, M., and Volk, T. (1996). A *Drosophila* dystrophin-related protein, MSP-300, is required for embryonic muscle morphogenesis. Mech. Dev. *60*, 83–94.

Soullam, B., and Worman, H. J. (1995). Signals and structural features involved in integral membrane protein targeting to the inner nuclear membrane. J. Cell Biol. *130*, 15–27.

Starr, D. A., and Han, M. (2002). Role of ANC-1 in tethering nuclei to the actin cytoskeleton. Science *298*, 406–409.

Starr, D. A., and Han, M. (2003). ANChors away: an actin based mechanism of nuclear positioning. J. Cell Sci. *116*, 211–216.

Sullivan, T., Escalante-Alcalde, D., Bhatt, H., Anver, M., Bhat, N., Nagashima, K., Stewart, C. L., and Burke, B. (1999). Loss of A-type lamin expression compromises nuclear envelope integrity leading to muscular dystrophy. J. Cell Biol. *147*, 913–920.

Tsuchiya, Y., Hase, A., Ogawa, M., Yorifuji, H., and Arahata, K. (1999). Distinct regions specify the nuclear membrane targeting of emerin, the responsible protein for Emery-Dreifuss muscular dystrophy. Eur. J. Biochem. *259*, 859–865.

Vaughan, O. A., Alvarez-Reyes, M., Bridger, J. M., Broers, J.L.V., Ramaekers, F.C.S., Wehnert, M., Morris, G. E., Whitfield, W.G.F., and Hutchison, C. J. (2001). Both emerin and lamin C depend on lamin A for localization at the nuclear envelope. J. Cell Sci. *114*, 2577–2590.

Venables, R. S., McLean, S., Luny, D., Moteleb, E., Morley, S., Quinlan, R. A., Lane, E. B., and Hutchison, C. J. (2001). Expression of individual lamins in basal cell carcinomas of the skin. Br. J. Cancer *84*, 512–519.

Worman, H. J., and Courvalin, J. C. (2002). The nuclear lamina and inherited disease. Trends Cell Biol. *12*, 591–598.

Ye, Q., and Worman, H. J. (1995). Protein-protein interactions between human nuclear lamins expressed in yeast. Exp. Cell Res. *219*, 292–298.

Zhang, Q., Skepper, J. N., Yang, F., Davies, J. D., Hegyi, L., Roberts, R. G., Weissberg, P. L., Ellis, J. A., and Shanahan, C. N. (2001). Nesprins: a novel family of spectrin-repeat-containing proteins that localize to the nuclear membrane in multiple tissues. J. Cell Sci. *114*, 4485–4498.

Zhang, Q., Ragnauth, C., Greener, M. J., Shanahan, C. M., and Roberts, R. G. (2002). The nesprins are giant actin-binding proteins, orthologous to *Drosophila melanogaster* muscle protein MSP-300. Genomics *80*, 473–481.

Zhang, Q., Ragnauth, C. D., Skepper, J. N., Worth, N. F., Warren, D. T., Roberts, R. G., Weissberg, P. L., Ellis, J. A., and Shanahan, C. M. (2005). Nesprin-2 is a multi-isomeric protein that binds lamin and emerin at the nuclear envelope and forms a subcellular network in skeletal muscle. J. Cell Sci. *118*, 673–687.

Zhen, Y. Y., Libotte, T., Munck, M., Noegel, A. A., and Korenbaum, E. (2002). NUANCE, a giant protein connecting the nucleus and actin cytoskeleton. J. Cell Sci. *115*, 3207–3222.